Supporting Information

Supramolecular Complex Strategy for Pure Organic Multi-Color Luminescent Materials and Stimuli-Responsive Luminescence Switching

Yue Shen, [a, b, ‡] Shiyin Wang, [a, ‡] Xiangyu Zhang, [a] Nan Li, [c] Haichao Liu*[a] and Bing Yang*[a]

[a.] State Key Laboratory of Supramolecular Structure and Materials, College of Chemistry, Jilin University, Changchun, 130012, P. R. China.

[b.] College of Science, Shenyang University of Chemical Technology, Shenyang, 110142, P. R. China.

[c.] College of Chemistry, Jilin University, Changchun, 130012, P. R. China.

Corresponding author e-mails: hcliu@jlu.edu.cn; yangbing@jlu.edu.cn.

‡These authors contributed equally.

S-Ⅰ. Experimental details

Materials:

All the reagents and solvents were purchased from commercial sources and used directly without further purification.

Synthesis:

9-Phenylacetylene anthracene (PEA) was synthesized according to a previous report.[1] The PEA crystals were prepared by dissolving PEA in mixed dichloromethane/methanol (2:1, v:v) solvents in a 10 mL tube, and the tube was kept at room temperature for several days to harvest yellow stripe-like crystal after the solvent partly evaporated. For the preparation of PEA-octafluoronaphthalene (PEA-OFN) and PEA-1,2,4,5-tetracyanobenzene (PEA-TCNB) crystals, PEA and OFN (1:1, mol:mol) were mixed and dissolved in mixed dichloromethane/methanol (2:1, v:v) solvents in a 10 mL tube at room temperature, and then colorless needle-like co-crystals were precipitated after the solvent partly evaporated, and PEA-TCNB co-crystals were obtained following the same method. It is worth noting that the solvents are different. In this case, mixed solvents of dichloromethane/acetonitrile (1:1, v:v) was chosen, and then red block co-crystals were harvested.

General information:

^{1}H NMR spectra were recorded on a Bruker AVANCE 500 spectrometer at room temperature, using tetramethylsilane (TMS) as the internal standard.

UV-vis absorption spectra of solutions were recorded on a PE Lambda 365 Spectrophotometer. UV-vis spectra of crystals were recorded on a Lambda 950 UV/Vis/NIR Spectrophotometer, and barium sulfate was used as reflective medium. Crystals were fixed on the surface of compacted barium sulfate, and collected diffuse reflection spectrum (DRS) spectra were directly transformed into absorption spectrum. Photoluminescence (PL) spectra and time-resolved PL spectra were collected on an Edinburgh FLS980 Spectrometer. The PL quantum yields (PLQYs) were measured

absolutely using an integrating sphere on an Edinburgh FLS920 Spectrometer. The excitation wavelength in PLQYs measurements was monitored at 380 nm for tetrahydrofuran (THF) solution. The excitation wavelength in PLQYs measurements was monitored at 380 nm, 400 nm, and 550 nm for PEA-OFN crystal, PEA crystal, and PEA-TCNB crystal, respectively. Time-resolved PL spectra were recorded on an Edinburgh FLS980 Spectrometer by using time-correlated single photon counting method under the excitation of EPL 375 laser with 68.9 ps pulse width.

The average lifetimes of multi-sectioned PL-decay spectra are calculated using the following equation:

$$\tau = \frac{\sum_{i=1}^{n} \tau_i^2 A_i}{\sum_{i=1}^{n} \tau_i A_i}$$

where τ is the lifetime, i represents the number of the lifetime components, and A_i is the proportion for each lifetime components.

The X-ray diffraction (XRD) data were collected on a Rigaku R-AXIS RAPID diffractometer equipped with Mo-Kα radiation (λ = 0.71073 Å), and the crystal structures were solved with a SHELXTL program and refined anisotropically using a full-matrix least-squares procedure. Interplanar distance of molecular planes and dihedral were measured using Mercury 3.9 Version software. Powder XRD (PXRD) patterns were collected on a Rigaku SmartLab(3) diffractometer.

Differential scanning calorimetry (DSC) analysis was carried out using a NETZSCH (DSC-204) instrument at 10 °C min^{-1} while flushing with nitrogen. Thermal gravimetric analysis (TGA) was undertaken on a PerkinElmer thermal analysis system at a heating rate of 10 °C min^{-1} and a nitrogen flow rate of 80 mL min^{-1}.

Theoretical calculations:

All the calculations were performed using Gaussian 09 (version D.01) package[2] on a Power Leader cluster. The highest occupied molecular orbital (HOMO) and the

lowest unoccupied molecular orbital (LUMO) were obtained by density functional theory (DFT) at the level of M06-2X/6-31G (d, p). The excitation energies and natural transition orbitals (NTOs) were performed by the time-dependent density function theory (TD-DFT) calculations at the level of M06-2X/6-31G (d, p). Intermolecular interactions were simulated by Multiwfn Software.[3] Transition density matrix (TDM) maps were obtained by Multiwfn Software. The interaction energies of three bimolecular models based on the geometries in crystals, were estimated at the level of M06-2X/6-31G (d, p).

S-Ⅱ. Figures and Tables

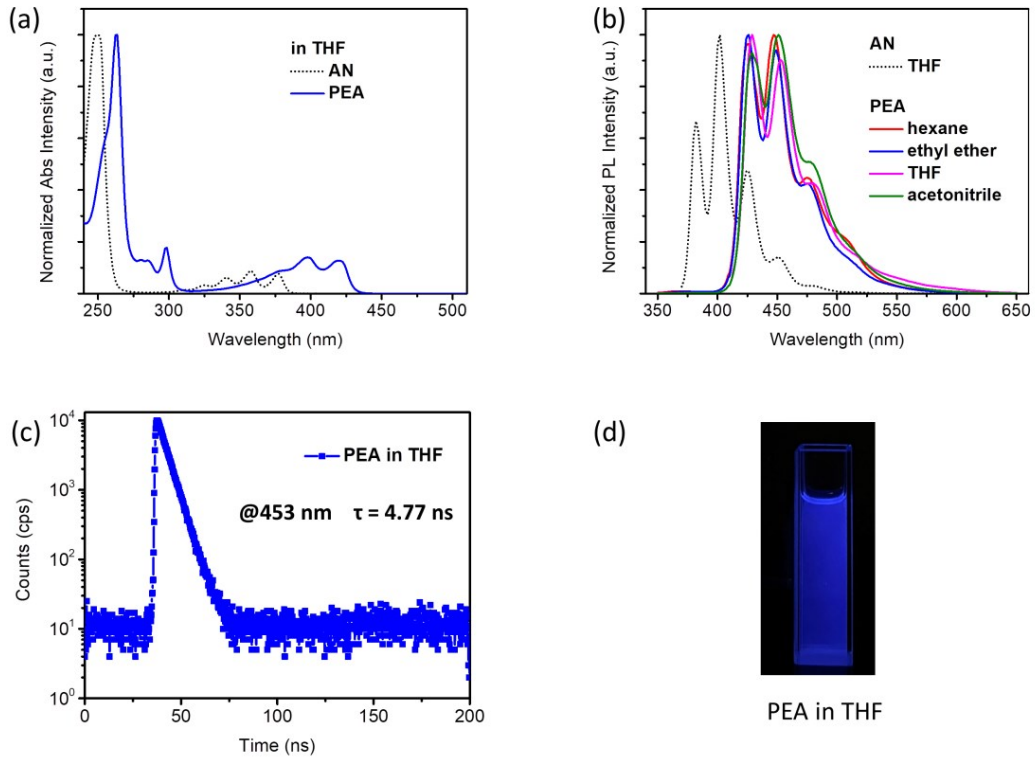

Fig. S1 (a) Absorption spectra of anthracene (AN) and PEA in THF solvent. (b) PL spectra of AN in THF solvent and PEA in different solvents. (c) Time-resolved PL spectrum and (d) photograph of PEA in THF solvent.

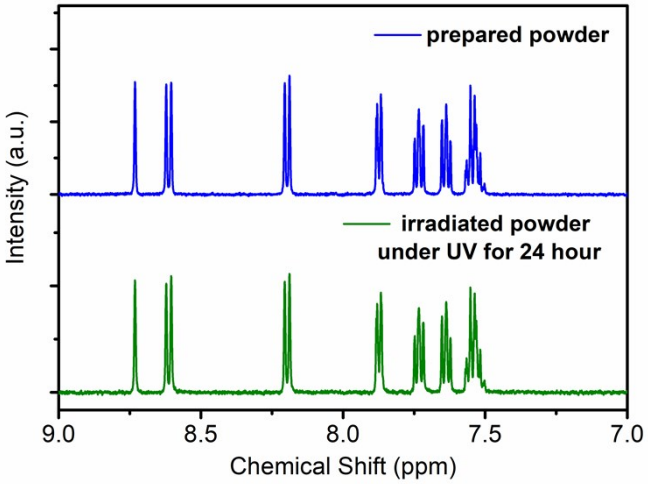

Fig. S2 ^{1}H NMR spectra of prepared and irradiated powders of PEA.

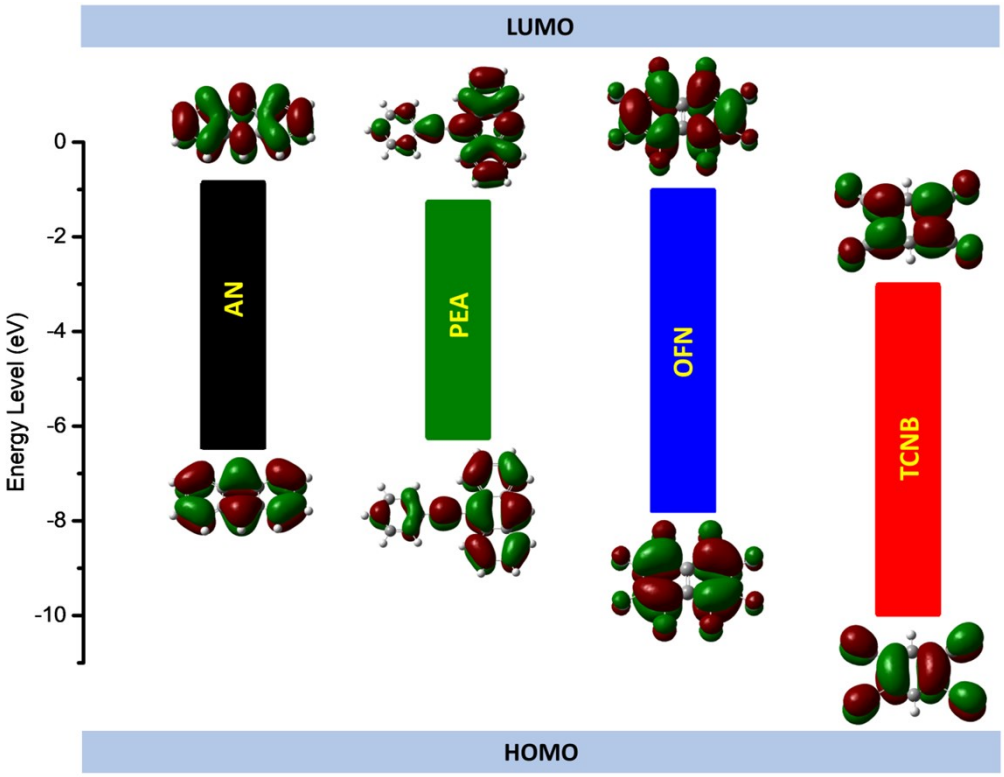

Fig. S3 HOMO and LUMO of AN, PEA, OFN, and TCNB by theoretical calculations.

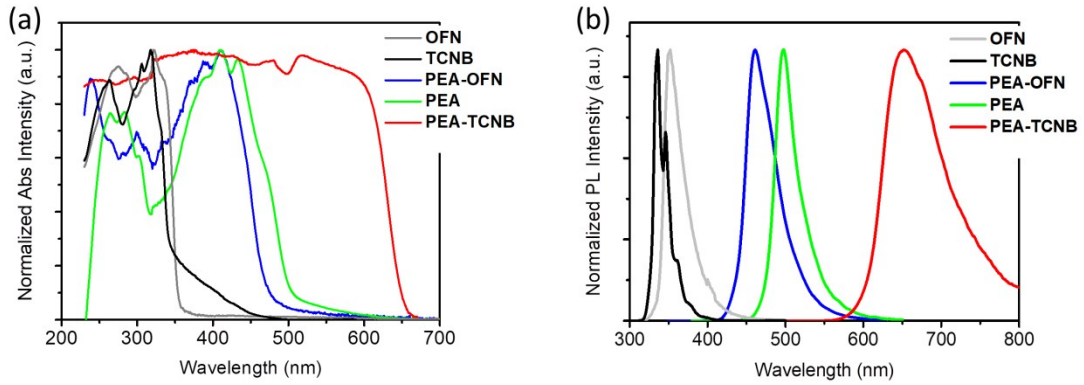

Fig. S4 (a) Absorption and (b) PL spectra of OFN, TCNB, PEA-OFN, PEA, and PEA-TCNB crystals.

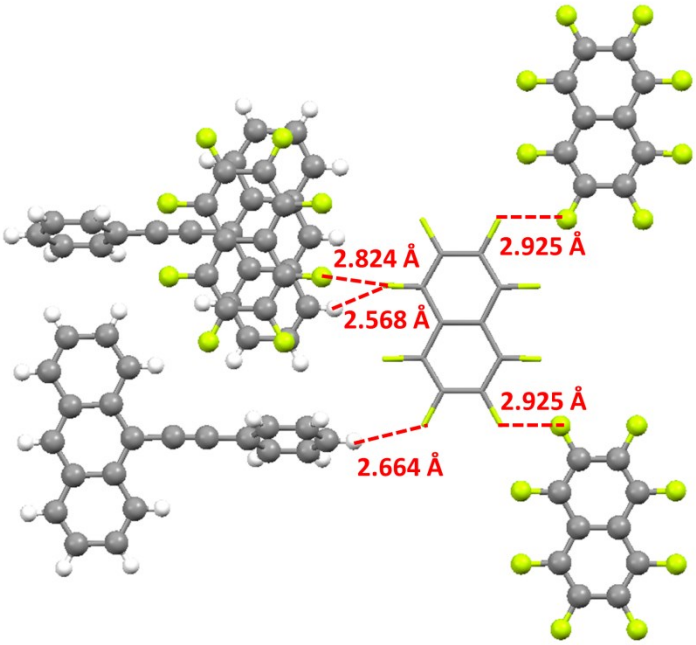

Fig. S5 Intermolecular interactions surrounding OFN molecule in PEA-OFN crystal.

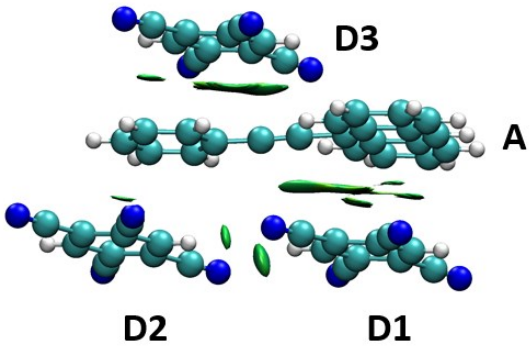

Fig. S6 Diagram of intermolecular interactions in PEA-TCNB crystal by Multiwfn software.

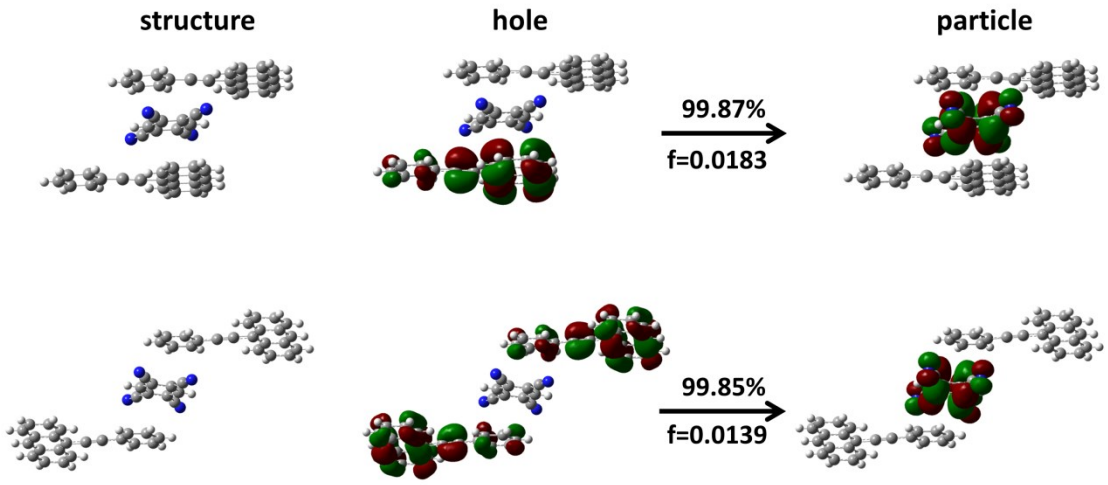

Fig. S7 Structures and corresponding NTOs in PEA-TCNB crystal.

According to the crystal structure of PEA-TCNB, there are three TCNB molecules around PEA. Theoretical calculations of intermolecular interactions and NTOs demonstrate that the fluorescence mainly origins from the AN unit and its adjacent TCNB molecule. Obviously, there are much stronger π-π interactions between D1 and A moieties in **Figure S6**. Thus, these two molecules are chosen as a model to calculate the relevant information.

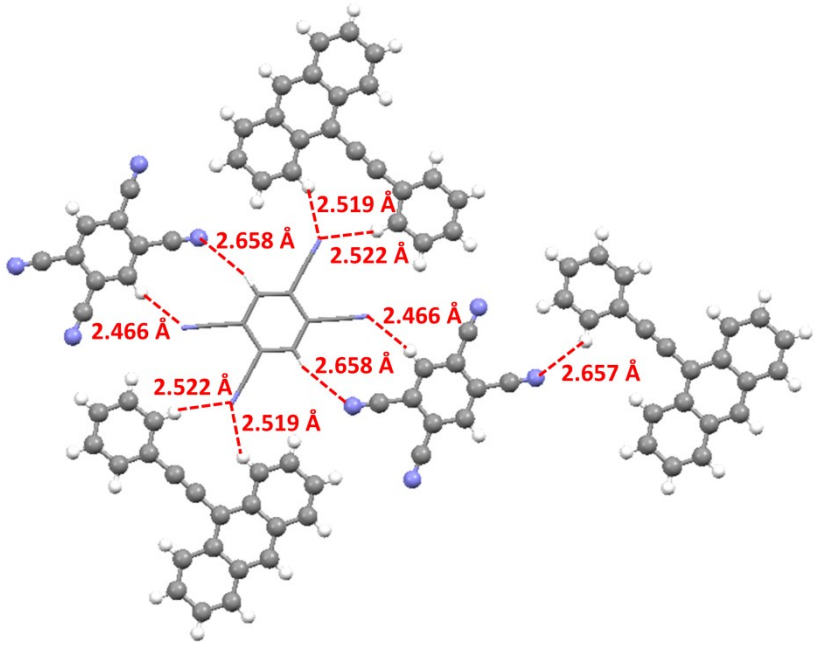

Fig. S8 Intermolecular interactions in PEA-TCNB crystal.

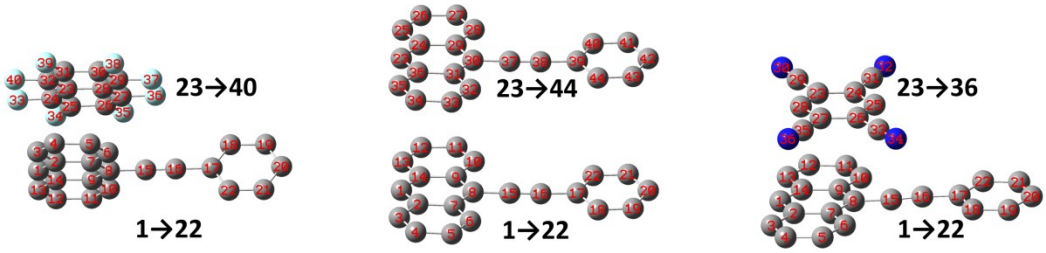

Fig. S9 Labeled atoms for the calculation of TDM map of dimer. Since hydrogen atoms usually have little contribution to the transitions we are interested in, they are usually ignored by default.

For the two-dimension (2D) color-filled map, both the horizontal axis x_i and the vertical axis y_i run over all of the non-hydrogen atoms of dimer. Each coordinate point (x_i, y_i) is related to the probability $|\Psi(x_i, y_i)|^2$ of finding the electron and hole in the π-atomic orbitals of two non-hydrogen atoms x_i and y_i, respectively. The brightness of each coordinate point (x_i, y_i) is directly proportional to the probability of $|\Psi(x_i, y_i)|^2$. The area of diagonal of 2D color-filled map represents that electronic transition has a dominant locally-excited (LE) character, while the area of off-diagonal represents a charge-transfer (CT) character.

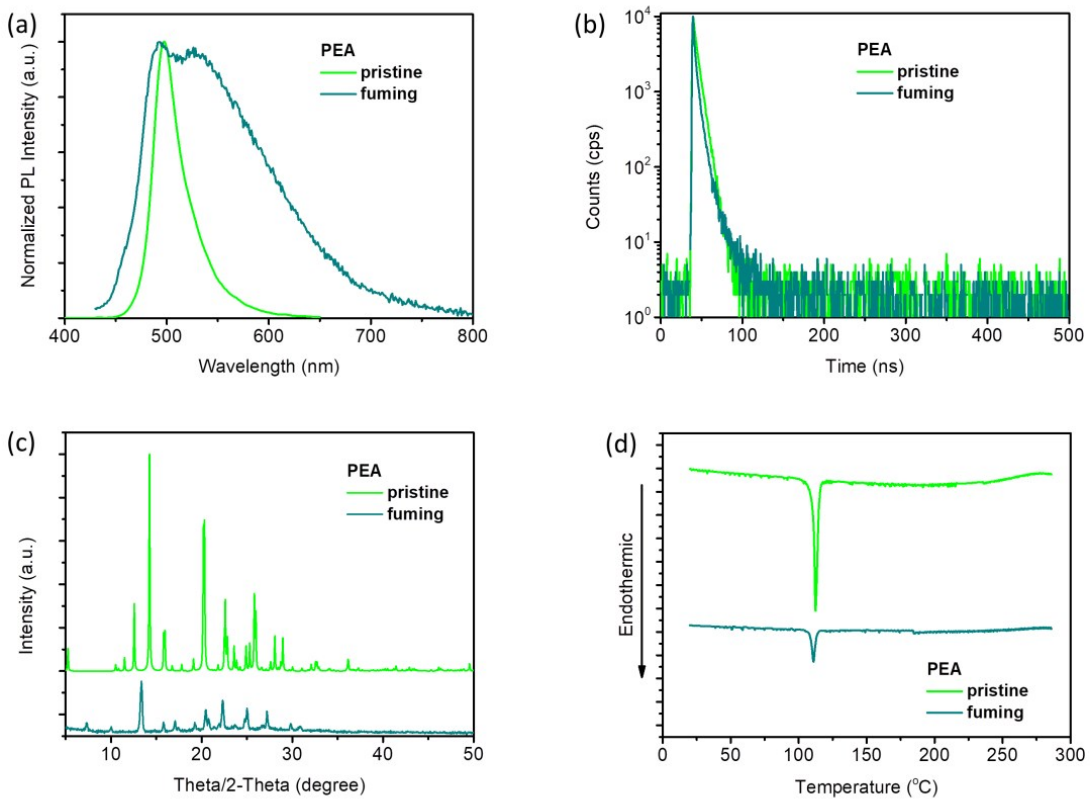

Fig. S10 (a) PL spectra, (b) time-resolved PL spectra, (c) PXRD patterns, and (d) DSC curves of ground PEA crystals after fuming treatment.

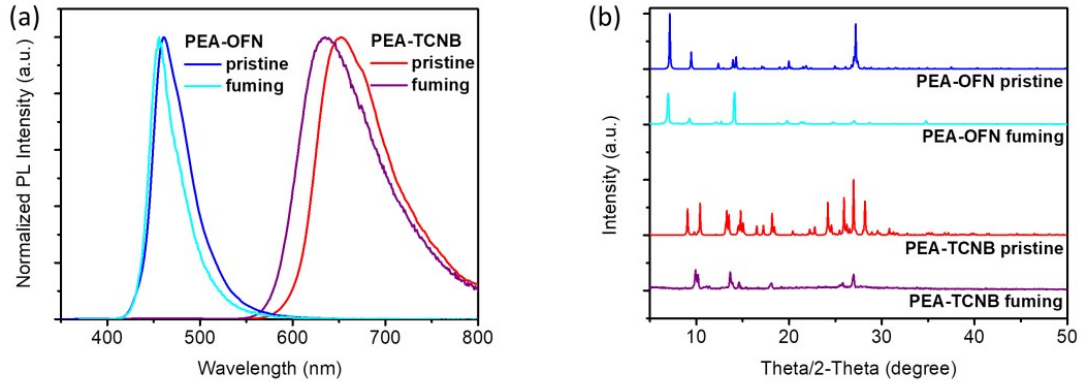

Fig. S11 (a) PL spectra and (b) PXRD patterns of ground PEA-OFN and PEA-TCNB crystals after fuming treatment.

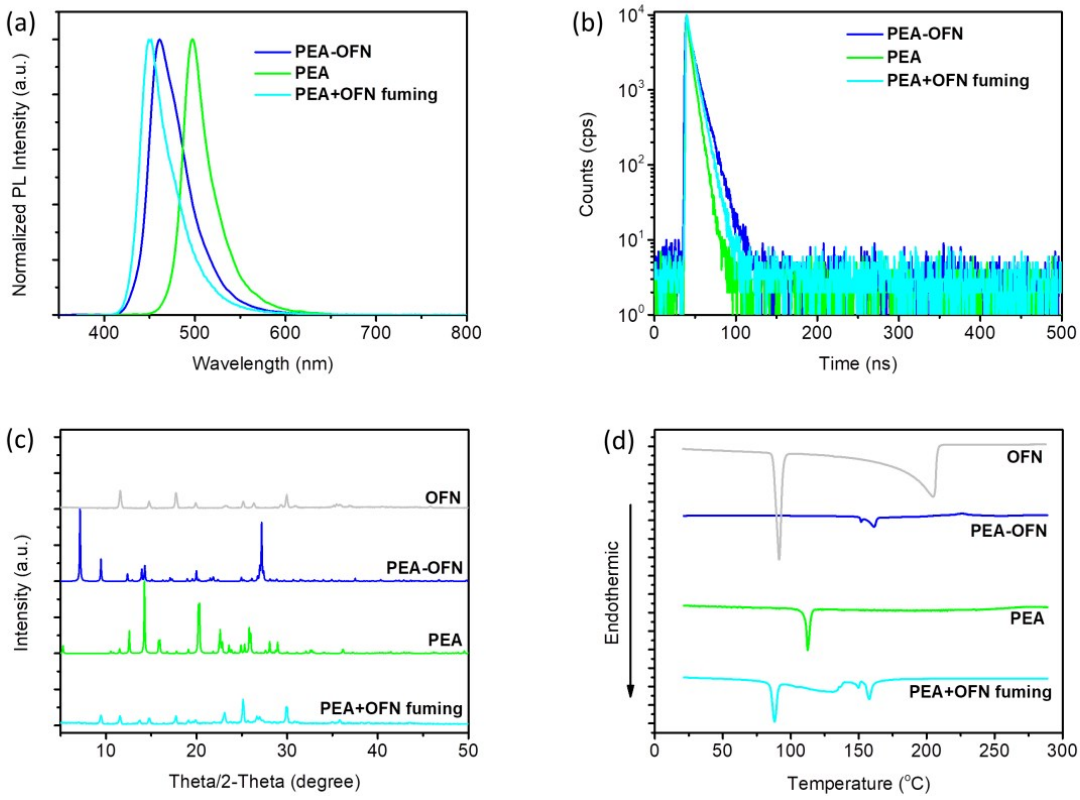

Fig. S12 (a) PL spectra, (b) time-resolved PL spectra, (c) PXRD patterns, and (d) DSC curves of ground binary mixture of PEA and OFN crystals after fuming treatment.

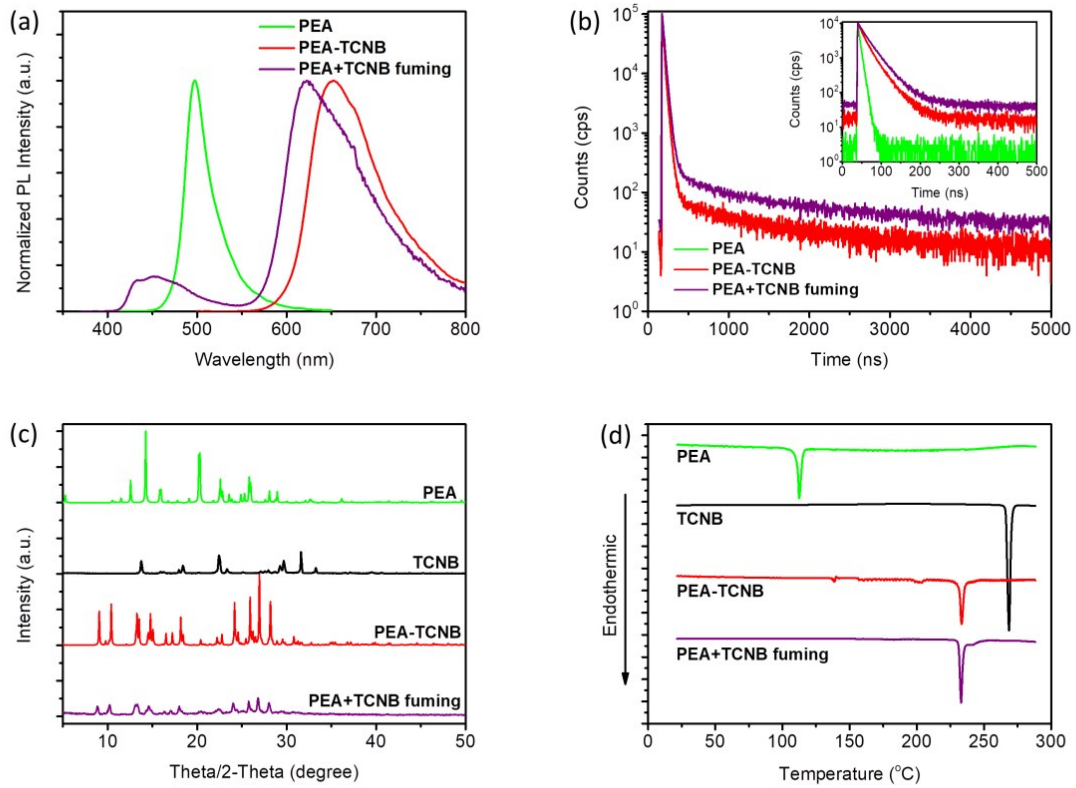

Fig. S13 (a) PL spectra, (b) time-resolved PL spectra, (c) PXRD patterns, and (d) DSC curves of ground binary mixture of PEA and TCNB crystals after fuming treatment. PEA-TCNB crystal shows the thermally activated delayed fluorescence (TADF) properties.

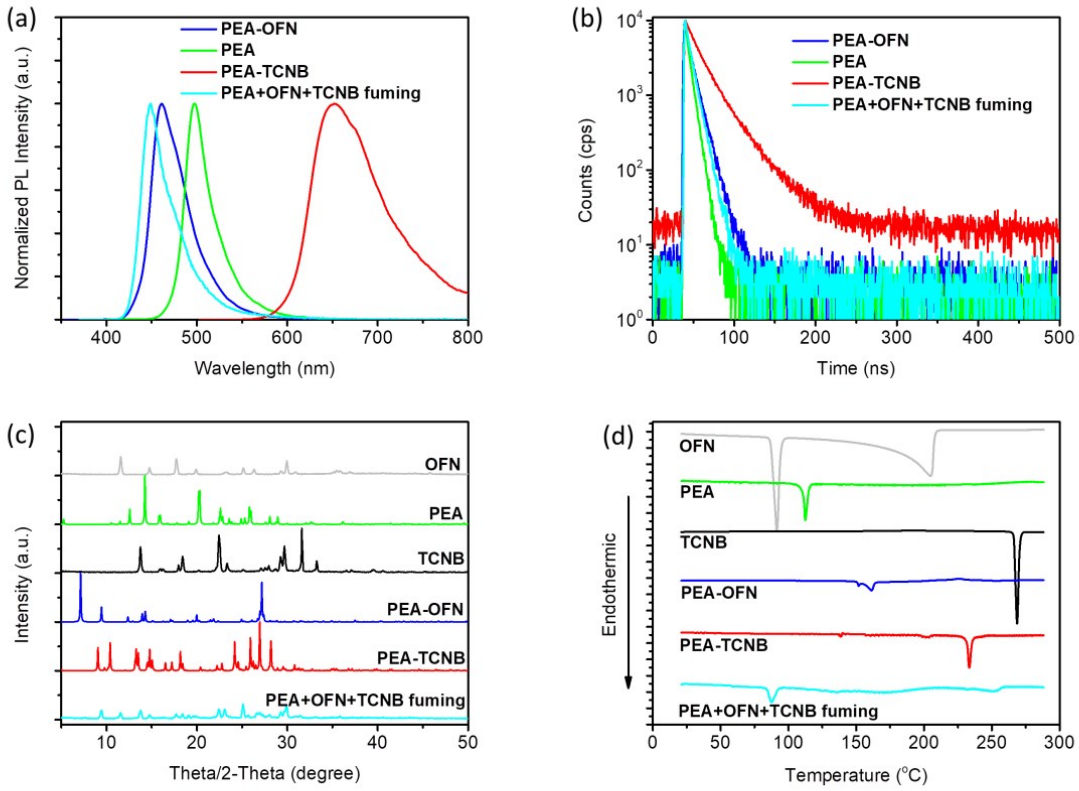

Fig. S14 (a) PL spectra, (b) time-resolved PL spectra, (c) PXRD patterns, and (d) DSC curves of ground ternary mixture of PEA, OFN, and TCNB crystals after fuming treatment.

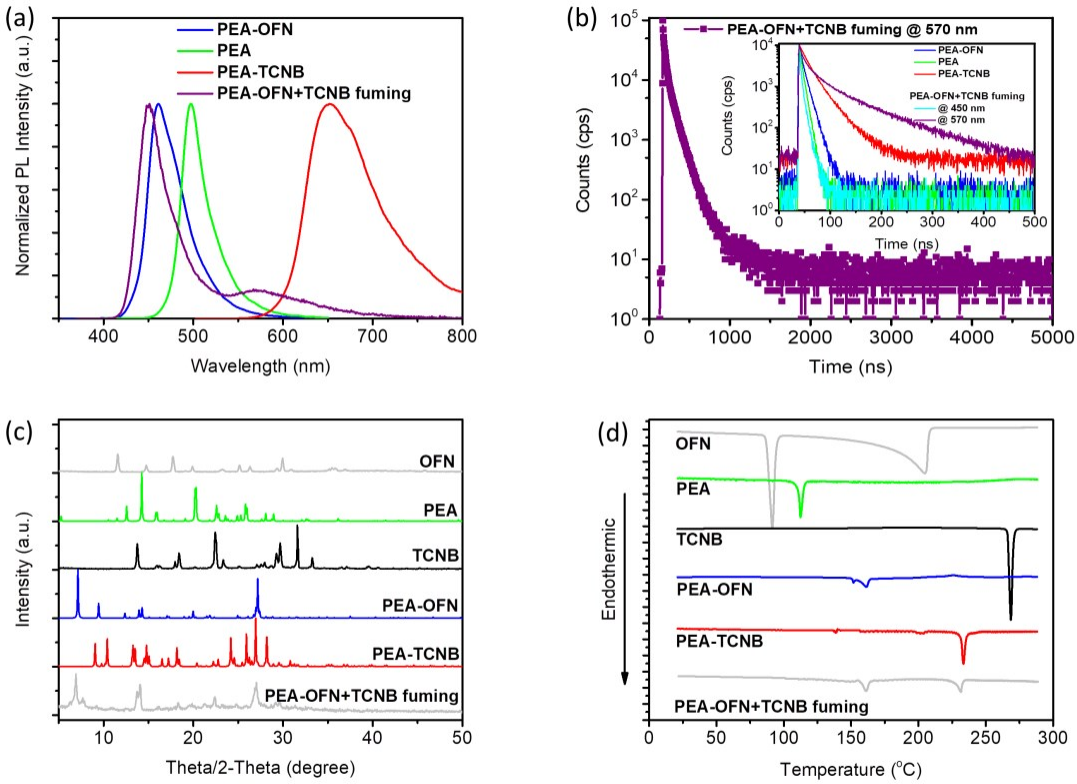

Fig. S15 (a) PL spectra, (b) time-resolved PL spectra, (c) PXRD patterns, and (d) DSC curves of ground mixture of PEA-OFN and TCNB crystals after fuming treatment.

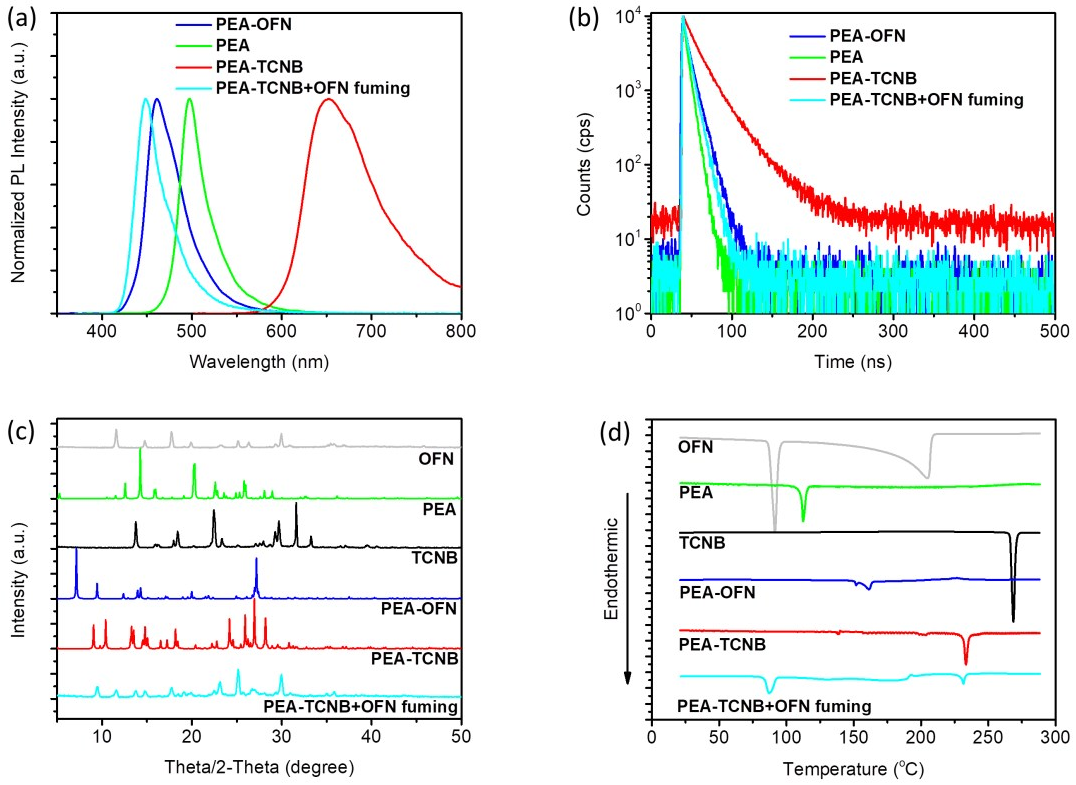

Fig. S16 (a) PL spectra, (b) time-resolved PL spectra, (c) PXRD patterns, and (d) DSC curves of ground mixture of PEA-TCNB and OFN crystals after fuming treatment.

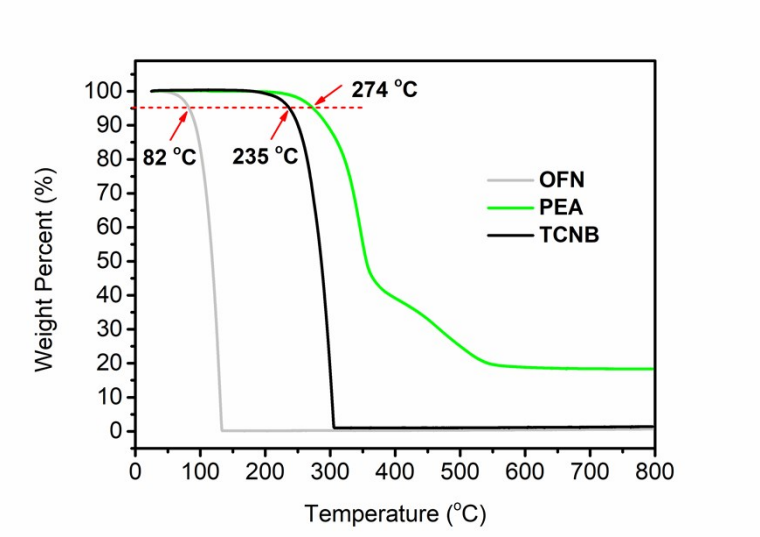

Fig. S17 TGA curves of OFN, PEA, and TCNB crystals.

Table S1. Photophysical data of PEA-OFN, PEA and PEA-TCNB crystals.

	λ_{max}[a] (nm)	τ[b] (ns)	goodness of fit (χ^2)	PLQY[c] (%)	rate constants[d] (s^{-1})
PEA-OFN	461	τ_{ave}=8.44 τ_1=4.37 (21.26%); τ_2=10.19 (78.74%)	0.998	51	$k_F=6.04\times10^7$ $k_{nr}=5.80\times10^7$
PEA	500	5.53	1.174	45	$k_F=8.14\times10^7$ $k_{nr}=9.95\times10^7$
PEA-TCNB	651	time scale: 500 ns τ_{ave}=25.90 τ_1=14.30 (50.70%); τ_2=31.21 (49.30%) time scale: 5000 ns τ_1=12.10 (29.60%); τ_2=30.32 (61.96%); τ_3=994.1 (8.44%)	1.055 1.179	4	$k_F=1.46\times10^6$ $k_{TADF}=4.02\times10^4$ $k_{IC}=3.50\times10^7$ $k_{ISC}=3.36\times10^6$ $k_{RISC}=1.61\times10^3$

[a] λ_{max} is the maximum PL wavlength. [b]τ is the lifetime, and τ_{ave} is the average lifetime. τ_{ave} is calculated according to **S- Ⅰ Experimental details**. [c] PLQY is the PL quantum yield. [d] For non-TADF PEA-OFN and PEA crystals, k_F is the fluorescence radiation rate constant and k_{nr} is the nonradiation rate constant. For PEA-TCNB crystal with TADF properties, k_F is the prompt fluorescence radiation rate constant, k_{TADF} is the TADF rate constant, k_{IC} is the internal conversion (IC) rate constant, k_{ISC} is the intersystem crossing (ISC) rate constant, and k_{RISC} is the reverse intersystem crossing (RISC) rate constant.

Rate constants are calculated using the following equation:

for non-TADF PEA-OFN and PEA crystals,

$$PLQY = \frac{k_F}{k_F + k_{nr}}$$

$$\tau = \frac{1}{k_F + k_{nr}}$$

for PEA-TCNB crystal with TADF properties,

$$PLQY = \frac{k_F}{k_F + k_{IC}}$$

$$\Phi_F = \frac{k_F}{k_F + k_{IC} + k_{ISC}} = k_F \times \tau_F$$

$$\Phi_{ISC} = \frac{k_{ISC}}{k_F + k_{IC} + k_{ISC}}$$

$$k_{TADF} = \frac{\Phi_{TADF}}{\Phi_{ISC} \times \tau_{TADF}}$$

$$k_{RISC} = \frac{k_F \times k_{TADF} \times \Phi_{TADF}}{k_{ISC} \times \Phi_F}$$

where Φ_F is the prompt fluorescence efficiency, Φ_{ISC} is the ISC efficiency, Φ_{TADF} is the TADF efficiency, τ_F is prompt fluorescence lifetime, and τ_{TADF} is delayed lifetime. Φ_F and Φ_{TADF} are calculated using PLQY multiplied by the proportion of each component.

Table S2. Crystallographic data of PEA-OFN, PEA, and PEA-TCNB crystals.

	PEA-OFN	PEA	PEA-TCNB
crystal color	colorless	yellow	red
empirical formula	$C_{32}H_{14}F_8$	$C_{22}H_{14}$	$C_{37}H_{17}N_6$
formula weight	550.43	278.33	545.56
T [K]	293(2)	293(2)	293(2)
crystal system	monoclinic	monoclinic	monoclinic
space group	P 1 21/c 1	P 21/c	P 1 21/c 1
a [Å]	6.8012(4)	16.900(2)	9.7595(5)
b [Å]	24.7708(15)	5.5710(7)	7.9919(3)
c [Å]	14.5619(9)	16.420(2)	36.1641(16)
α [°]	90	90	90
β [°]	101.513(2)	96.441(4)	91.4780(18)
γ [°]	90	90	90
V [Å^3]	2403.9(3)	1536.2(3)	2819.8(2)
Z	4	4	4
F(000)	1112	584	1124
density [g/cm^3]	1.521	1.203	1.285
μ [mm^{-1}]	0.131	0.068	0.079
reflections collected	40935	11878	55890
unique reflections	5120	2705	6962
R (int)	0.0662	0.0779	0.0650
GOF	1.074	1.091	1.066
R_1 [$I>2\sigma(I)$]	0.0784	0.0779	0.0668
ωR_2 [$I>2\sigma(I)$]	0.1464	0.1928	0.1336
R_1 (all data)	0.1417	0.1999	0.1199
$\omega R2$ (all data)	0.1760	0.3051	0.1608
CCDC number	2075152	2075150	2075151

S-Ⅲ. Reference

[1] C.-W. Wan, A. Burghart, J. Chen, F. Bergström, L. B.-Å. Johansson, M. F. Wolford, T. GyumKim, M. R. Topp, R. M. Hochstrasser and K. Burgess, *Chem. Eur. J.*, 2003, **9**, 4430-4441.

[2] M. J. Frisch, G. W. Trucks, H. B. Schlegel, G. E. Scuseria, M. A. Robb, J. R. Cheeseman, G. Scalmani, V. Barone, B. Mennucci, G. A. Petersson, H. Nakatsuji, M. Caricato, X. Li, H. P. Hratchian, A. F. Izmaylov, J. Bloino, G. Zheng, J. L. Sonnenberg, M. Hada, M. Ehara, K. Toyota, R. Fukuda, J. Hasegawa, M. Ishida, T. Nakajima, Y. Honda, O. Kitao, H. Nakai, T. Vreven, J. A. Montgomery, Jr., J. E. Peralta, F. Ogliaro, M. Bearpark, J. J. Heyd, E. Brothers, K. N. Kudin, V. N. Staroverov, T. Keith, R. Kobayashi, J. Normand, K. Raghavachari, A. Rendell, J. C. Burant, S. S. Iyengar, J. Tomasi, M. Cossi, N. Rega, J. M. Millam, M. Klene, J. E. Knox, J. B. Cross, V. Bakken, C. Adamo, J. Jaramillo, R. Gomperts, R. E. Stratmann, O. Yazyev, A. J. Austin, R. Cammi, C. Pomelli, J. W. Ochterski, R. L. Martin, K. Morokuma, V. G. Zakrzewski, G. A. Voth, P. Salvador, J. J. Dannenberg, S. Dapprich, A. D. Daniels, O. Farkas, J. B. Foresman, J. V. Ortiz, J. Cioslowski, and D. J. Fox, *Gaussian 09, Revision D.01*, Gaussian, Inc., Wallingford CT, 2013.

[3] T. Lu, F. Chen, *J. Comput. Chem.*, 2012, **33**, 580-592.